COMPOSITION DEPENDENCE OF THE BAND GAP ENERGY OF $In_xGa_{1-x}N$ LAYERS ON GaN (x≤0.15) GROWN BY METAL-ORGANIC CHEMICAL VAPOR DEPOSITION

J. Wagner, A. Ramakrishnan, D. Behr, M. Maier, N. Herres, M. Kunzer, H. Obloh, and K.-H. Bachem

Fraunhofer-Institut für Angewandte Festkörperphysik, Tullastrasse 72, D-79108 Freiburg, Germany, wagner@iaf.fhg.de

Cite this article as: MRS Internet J. Nitride Semicond. Res. 4S1, G2.8 (1999)

ABSTRACT

We report on the composition dependence of the band gap energy of strained hexagonal $In_xGa_{1-x}N$ layers on GaN with x≤0.15, grown by metal-organic chemical vapor deposition on sapphire substrates. The composition of the (InGa)N was determined by secondary ion mass spectroscopy. High-resolution X-ray diffraction measurements confirmed that the (InGa)N layers with typical thicknesses of 30 nm are pseudomorphically strained to the in-plane lattice parameter of the underlying GaN. Room-temperature photoreflection spectroscopy and spectroscopic ellipsometry were used to determine the (InGa)N band gap energy. The composition dependence of the band gap energy of the strained (InGa)N layers was found to be given by $E_G(x)=3.43-3.28\cdot x$ (eV) for x≤0.15. When correcting for the strain induced shift of the fundamental energy gap, a bowing parameter of 3.2 eV was obtained for the composition dependence of the gap energy of unstrained (InGa)N.

INTRODUCTION

There is considerable current interest in the (InGa)N alloy system because (InGa)N layers form the active region of most of the present green-to-violet light emitting devices based on group III-nitrides [1]. However, in spite of the technological importance of (InGa)N, so far published data on the composition dependence of the band gap energy of the (InGa)N alloy show significant scatter, with values for the bowing parameter ranging from 1.02 eV [2] to 3.5 eV [3].

For an accurate determination of the composition dependence of the (InGa)N band gap, the gap energy has to be derived from photoreflection (PR) [2] or spectroscopic ellipsometry (SE) [4] measurements rather than from photoluminescence (PL) data. This is because the (InGa)N near band-edge PL spectrum is Stokes-shifted relative to the band edge, leading to an underestimate of the gap energy [5]. The (InGa)N alloy composition should be assessed not only by X-ray diffraction but also by chemical analysis, as strain effects complicate the composition analysis by X-ray diffraction, requiring precise knowledge of the elastic parameters of the (InGa)N. (InGa)N layers grown on top of GaN have been found to be strained to the in-plane lattice parameter of the underlying GaN for layer thicknesses and compositions up to, at least, 100 nm and x=0.15, respectively [6,7].

In the present study pseudomorphically strained (InGa)N layers on GaN, grown by metal-organic chemical vapor deposition (MOCVD), were analyzed by PR spectroscopy and SE to determine the composition dependence of the (InGa)N band gap energy. Secondary ion mass spectroscopy (SIMS) and high-resolution X-ray diffraction (HRXRD) were used to assess the (InGa)N layers` composition and strain, respectively.

https://doi.org/10.1557/S1092578300002301 Published online by Cambridge University Press

EXPERIMENT

The hexagonal (InGa)N-on-GaN samples used in this study were grown by low-pressure MOCVD on c-plane 2´´ sapphire substrates. Details on growth can be found in Ref. 8. Data will be presented on a series of samples with varying In content ($x \leq 0.15$) and (InGa)N layer thicknesses ranging from 15 to 60 nm, grown on top of a 2 to 3 µm thick GaN layer. The (InGa)N composition was determined by SIMS using appropriate standards calibrated by energy dispersive X-ray analysis (EDX).

Selected samples were further analyzed by HRXRD using both the symmetric 00.6 and the asymmetric 10.5 reflections, in order to determine the *c* and *a* lattice parameters parallel and perpendicular to the growth axis. Fig. 1 shows a plot of *c* versus *a* for (InGa)N layers with a thickness of 30 nm as well as for the underlying GaN. All the *a* lattice parameters obtained for the (InGa)N are close to that of the GaN layer, indicating that the (InGa)N layers are under biaxial in-plane compression due to pseudomorphic growth. The GaN layer itself is also under slight compression due to the thermal mismatch with respect to the sapphire substrate. Using linear interpolations between the *c* and *a* lattice parameters of unstrained GaN [9] and InN [10], the composition dependent lattice parameters of unstrained (InGa)N are obtained, shown in Fig. 1 by the short-dashed line. Based on the elastic parameters given by Wright [11], the effect of in-plane biaxial

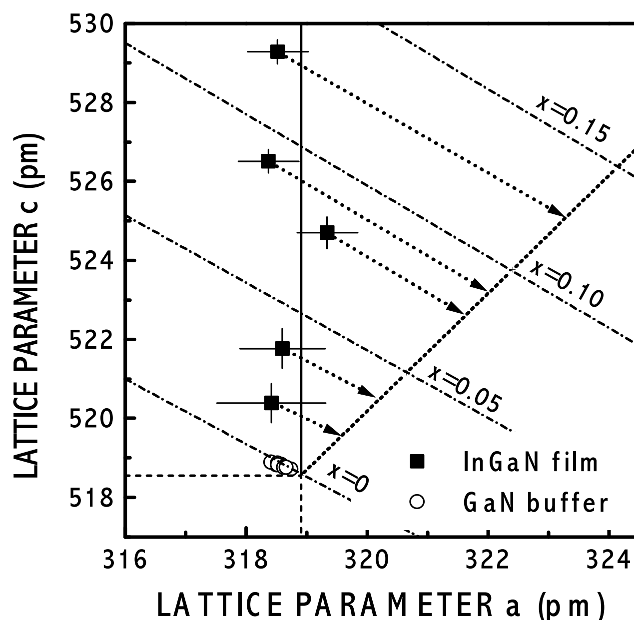

Fig. 1: c versus a lattice parameters as determined by HRXRD for 30 nm thick $In_xGa_{1-x}N$ layers on GaN (filled squares) with different In content x. Error bars are indicated. For comparison c and a lattice parameters of the underlying GaN are also shown (open circles). The full vertical line marks the a lattice parameter of unstrained GaN. The short-dashed line indicates the calculated c-versus-a relation for unstrained (InGa)N. For further details see text.

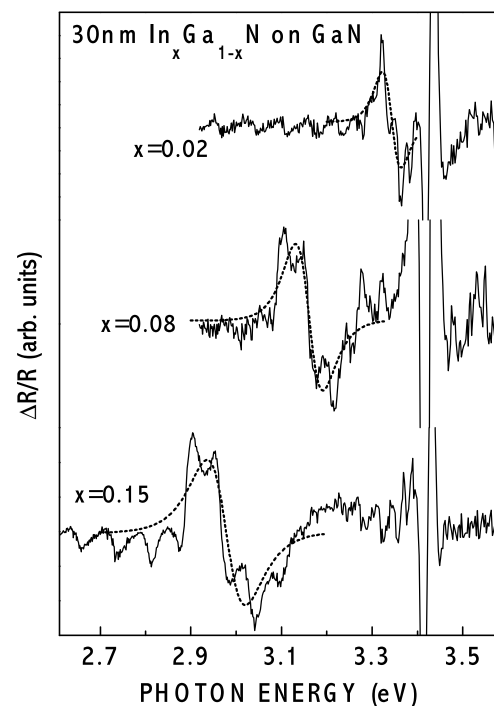

Fig. 2: Room-temperature PR spectra of 30 nm thick $In_xGa_{1-x}N$ layers on GaN with various In contents x given in the figure. Dashed curves indicate fits to the (InGa)N fundamental gap resonance.

https://doi.org/10.1557/S1092578300002301 Published online by Cambridge University Press

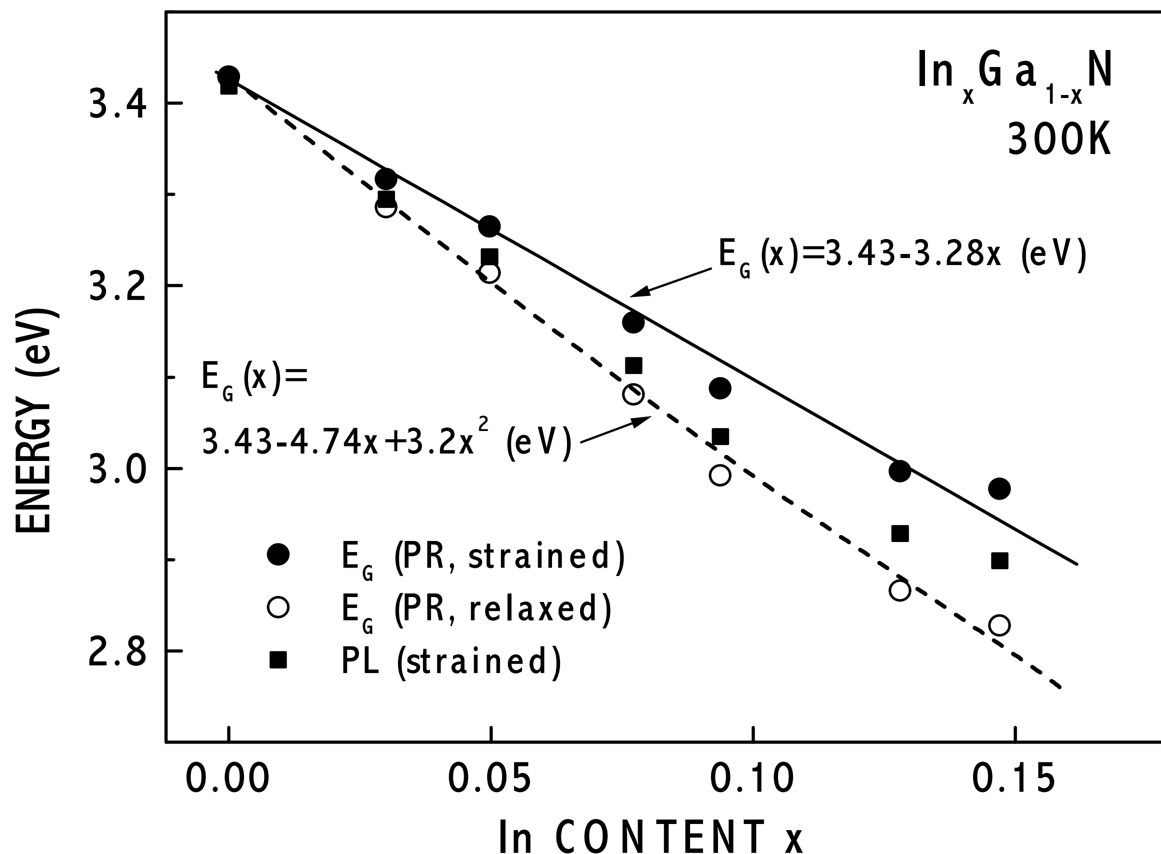

Fig. 3: Composition dependence of the room-temperature band gap energy of strained $In_xGa_{1-x}N$ layers on GaN as obtained by PR spectroscopy (filled circles), and after correction for the strain induced band gap shift (open circles, see text). (InGa)N alloy composition was determined by SIMS. The full and dashed curves indicate linear and quadratic fits to E_G for strained $In_xGa_{1-x}N$ and for numerically relaxed $In_xGa_{1-x}N$, respectively. For comparison, room-temperature PL peak positions are also shown (filled squares).

compressive or tensile strain on *c* and *a* can be calculated, as indicated by the dash-dotted lines for In contents of x=0, 0.05, 0.10, and 0.15. To extract information on the In content of the present strained (InGa)N layers, the measured data have to be projected parallel to the dash-dotted lines onto the *c*-versus-*a* curve for unstrained (InGa)N (short-dashed line), as indicated by arrows. The (InGa)N alloy composition deduced in this way agrees for x<0.1 within 10% with the SIMS data. For the highest In contents the HRXRD analysis yields a somewhat lower In content than SIMS, e.g. x=0.124 (HRXRD) versus x=0.147 (SIMS). Considering the large uncertainties in the (InGa)N elastic parameters required for the HRXRD based analysis of the alloy composition for strained (InGa)N, the SIMS data are used throughout the remaining paper.

RESULTS AND DISCUSSION

Room-temperature PR spectra are plotted in Fig. 2 for three different $In_xGa_{1-x}N$-on-GaN samples with an (InGa)N layer thickness of 30 nm and In contents of x=0.02, 0.08, and 0.15. Besides the very intense and spectrally sharp fundamental gap resonance of GaN at 3.43 eV, the corresponding resonance of the (InGa)N is well resolved at lower energies as a derivative-like structure. The (InGa)N resonance shows a low-energy shift and a significant broadening with increasing In con-

https://doi.org/10.1557/S1092578300002301 Published online by Cambridge University Press

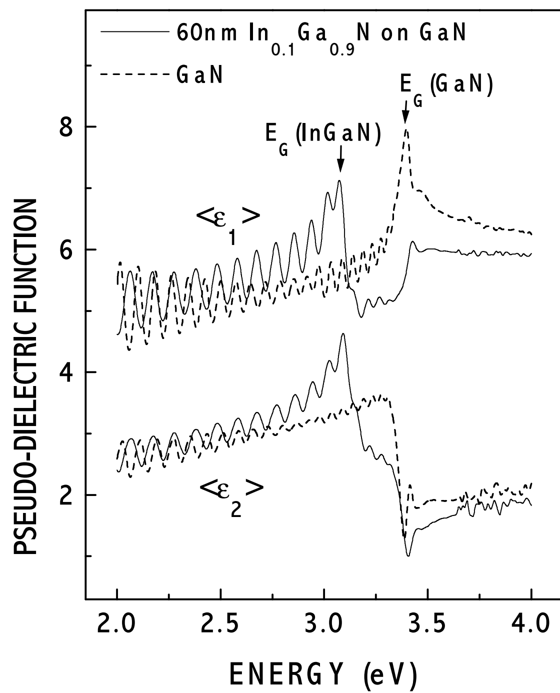

*Fig. 4: Real <**e**$_1$> and imaginary part <**e**$_2$> of the pseudo-dielectric function spectrum of a 60 nm thick $In_{0.1}Ga_{0.9}N$ layer on GaN and, for comparison, of a GaN reference sample. Data were derived from room-temperature SE measurements performed at an incident angle of 75° and a polarizer-azimuth of 30°.*

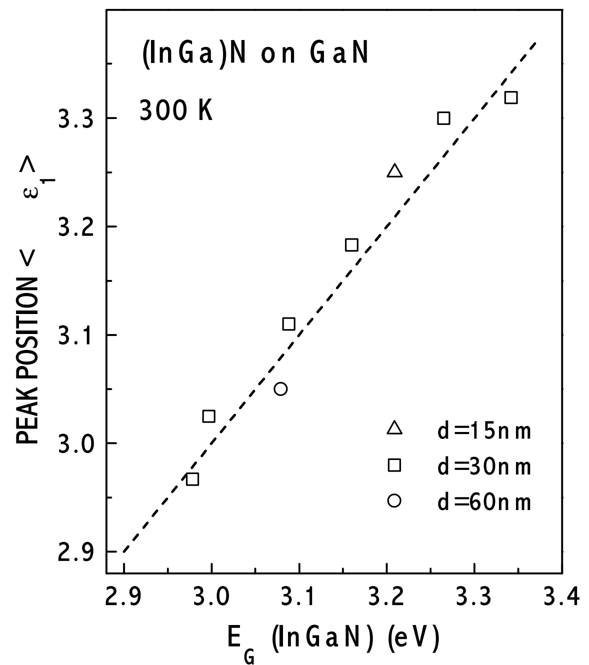

*Fig. 5: Energy position of the (InGa)N related peak in the <**e**$_1$> spectrum versus (InGa)N band gap energy derived from PR measurements. Data are shown for different (InGa)N layer thicknesses d given in the figure. The dashed line indicates a one-to-one correspondence.*

tent. Its line shape is somewhat distorted by Fabry-Perot interference oscillations. The band gap energy of the (InGa)N was deduced from a fit to the PR resonance [12], as shown by the dashed curves. The resulting band gap energies E_G are plotted in Fig. 3 versus the In content determined by SIMS (full circles). The experimental data can be fitted by the linear relationship $E_G(x)=3.43-3.28 \cdot x$ (eV) ($x \leq 0.15$), as indicated by the full line in Fig. 3. There is fair agreement with the composition dependence of the (InGa)N band gap energy reported by McClusky et al. [3] ($E_G(x)=3.42-3.93 \cdot x$ (eV)), which was obtained from optical transmission experiments on 0.25 µm thick $In_xGa_{1-x}N$ layers ($x \leq 0.12$) strained to the in-plane lattice parameter of the underlying GaN. For comparison the PL peak energy at room-temperature is also plotted in Fig. 3 (filled squares). There is an increasing Stokes-shift between the band gap energy derived from the PR measurements and the PL peak energy upon increasing the In content. Alloy fluctuations [5] and the confined Stark effect due to piezoelectric fields [14] have been discussed as possible mechanisms responsible for this Stokes-shift.

As pointed out by McClusky et al. [3], the strain induced shift ΔE of the (InGa)N band gap has to be subtracted from the present $E_G(x)$ data obtained on pseudomorphic (InGa)N films on GaN, to obtain the composition dependence of the band gap energy of <u>unstrained</u> (InGa)N. Using the relationship for the strain induced band gap shift $\Delta E=1.02 \cdot x$ (eV) given in Ref. 3, the expected band gap energies of unstrained (InGa)N have been calculated, which are shown in Fig. 3 by open circles. Taking a value of 1.89 eV for the room-temperature band gap energy of InN [15], the present data on the composition dependence of the band gap energy of unstrained (InGa)N

https://doi.org/10.1557/S1092578300002301 Published online by Cambridge University Press

can be fitted by $E_G(x)=3.43-4.74\cdot x+3.2\cdot x^2$ (eV). The bowing parameter of 3.2 eV compares favorably well with that of 3.5 eV calculated in Ref. 3 for x=0.125. There is also consistency with a very recent study by Wetzel et al. [16], which reports on the basis of a combined HRXRD and PR spectroscopic analysis a bowing parameter of 3.8 eV for unstrained $In_xGa_{1-x}N$ (x<0.2).

It has been shown recently that SE measurements allow a determination of the (InGa)N band gap energy too [4]. Fig. 4 shows the real $\langle\varepsilon_1\rangle$ and imaginary part $\langle\varepsilon_2\rangle$ of the pseudo-dielectric function of a 60 nm thick $In_{0.1}Ga_{0.9}N$-on-GaN layer. For comparison the pseudo-dielectric function spectrum of a high-quality bulk-like GaN reference layer is also shown, which is very similar to that reported in Ref. 17 for hexagonal GaN. A pronounced peak in $\langle\varepsilon_1\rangle$ and minimum in $\langle\varepsilon_2\rangle$ at 3.40 eV marks the superposition of the A and B excitonic transitions at the fundamental band gap of GaN [18,19]. At the high-energy side of this peak a shoulder appears in $\langle\varepsilon_1\rangle$ which is tentatively assigned to the C excitonic transition. The oscillations observed in the pseudo-dielectric function spectrum for photon energies below the fundamental energy gap are caused by Fabry-Perot interferences due to multiple internal reflections in the epitaxial layer. In the $\langle\varepsilon_1\rangle$ spectrum of the (InGa)N-on-GaN sample, the fundamental gap interband transition of the GaN is attenuated. A new peak appears in both $\langle\varepsilon_1\rangle$ and $\langle\varepsilon_2\rangle$ at about 3.07 eV, which is in the transparency region of the GaN. The new peak is assigned to the fundamental gap interband transition of the $In_{0.1}Ga_{0.9}N$.

This assignment is confirmed by a direct comparison of the energy position of the (InGa)N related peak in the $\langle\varepsilon_1\rangle$ spectrum with the band gap energy derived from the PR measurements. In Fig. 5 the (InGa)N peak position in $\langle\varepsilon_1\rangle$ is plotted versus the (InGa)N band gap energy for (InGa)N-on-GaN samples with In concentrations up to x=0.15 and (InGa)N layer thicknesses of 15, 30, and 60 nm. There is an almost one-to-one correspondence between these two quantities with the peak in $\langle\varepsilon_1\rangle$ being on the average only slightly higher in energy than the band gap.

CONCLUSION

The composition dependence of the band gap energy of strained $In_xGa_{1-x}N$ on GaN (x≤0.15) has been studied by PR spectroscopy and SE, using SIMS in combination with HRXRD for an accurate determination of the (InGa)N layers` composition and strain. The composition dependence of the band gap energy of (InGa)N strained to the in-plane lattice parameter of the underlying GaN was found to be given by $E_G(x)=3.43-3.28\cdot x$ (eV). After correction for the strain induced band gap shift, a bowing parameter of 3.2 eV was obtained for the composition dependence of the band gap of unstrained (InGa)N.

ACKNOWLEDGMENTS

Ch. Hoffmann and U. Kaufmann are thanked for performing the EDX analysis and for stimulating discussions, respectively. Continuous interest and encouragement by G. Weimann is gratefully acknowledged. Work was supported by the German Ministry for Education and Research.

REFERENCES

1. S. Nakamura and G. Fasol, *The Blue Laser Diode* (Springer, Berlin, 1997).
2. W. Shan, B. D. Little, J. J. Song, Z. C. Feng, M. Schurmann, and R. A. Stall, Appl. Phys. Lett. **69**, 3315 (1996).
3. M. D. McClusky, C. G. Van de Walle, C. P. Master, L. T. Romano, and N. M. Johnson, Appl. Phys. Lett. **72**, 2725 (1998).
4. J. Wagner, A. Ramakrishnan, D. Behr, H. Obloh, M. Kunzer, and K.-H. Bachem, Appl. Phys. Lett. **73**, 1715 (1998).

https://doi.org/10.1557/S1092578300002301 Published online by Cambridge University Press

5. S. Chichibu, T. Azuhata, T. Sota, and S. Nakamura, Appl. Phys. Lett. **70**, 2822 (1997).
6. H. Amano, T. Takeuchi, S. Sota, H. Sakai, and I. Akasaki, Mat. Res. Soc. Symp. Proc. Vol. **449**, 1143 (1997).
7. F. Scholz, J. Off, A. Kniest, L. Görgens, and O. Ambacher, in Proceedings of E-MRS Spring Meeting 1998, Symposium L *Nitrides and Related Wide Band Gap Materials* (to appear in Mat. Sci. Eng. B).
8. H. Obloh, D. Behr, N. Herres, C. Hoffmann, M. Kunzer, M. Maier, S. Müller, W. Pletschen, B. Santic, P. Schlotter, M. Seelmann-E., K.-H. Bachem, U. Kaufmann, Proc. 2nd Int. Conf. Nitride Semicond. (Tokushima, Japan, 1997), p. 258.
9. C. M. Balkas, C. Baskeri, and R. F. Davis, Powder Diffraction **10**, 266 (1995).
10. K. Kubota, Y. Kobayashi, and K. Fujimoto, J. Appl. Phys. **66**, 2984 (1989).
11. A. F. Wright, J. Appl. Phys. **82**, 2833 (1997).
12. D. E. Aspnes, Surf. Sci. **37**, 418 (1973).
13. C. M. Herzinger, P. G. Snyder, B. Johs, and J. A. Woollam, J. Appl. Phys. **77**, 1715 (1995).
14. T. Takeuchi, S. Sota, M. Katsurgawa, M. Komori, H. Takeuchi, H. Amano, and I. Akasaki, Jpn. J. Appl. Phys. **36**, L382 (1997); J. S. Im, H. Kollmer, J. Off, A. Sohmer, F. Scholz, and A. Hangleiter, Mat. Res. Soc. Symp. Proc. Vol. **482**, 513 (1998).
15. T. L. Tansley and C. P. Foley, J. Appl. Phys. **59**, 3241 (1986).
16. C. Wetzel, T. Takeuchi, S. Yamaguchi, H. Katoh, H. Amano, and I. Akasaki, Appl. Phys. Lett. **73**, 1994 (1998).
17. T. Kawashima, H. Yoshikawa, S. Adachi, S. Fuke, and K. Ohtsuka, J. Appl. Phys. **82**, 3528 (1997).
18. A.J. Fischer, W. Shan, J.J. Song, Y.C. Chang, R. Horning, and B. Goldenberg, Appl. Phys. Lett. **71**, 1981 (1997).
19. A.A. Yamaguchi, Y. Mochizuki, H. Sunakawa, and A. Usui, J. Appl. Phys. **83**, 4542 (1998).

https://doi.org/10.1557/S1092578300002301 Published online by Cambridge University Press